11. Rasulov, R. Y., Karimova, G. A., & Rahmatov, I. (2023). LINEAR-CIRCULAR DICHROISM OF THE PHOTON DRAG EFFECT IN SEMICONDUCTOR SUPERSTRUCTURES. Oriental renaissance: Innovative, educational, natural and social sciences, 3(4), 458-463.
12. Расулов, В. Р., Расулов, Р. Я., Исомаддинова, У. М., & Кодиров, Н. У. О. (2022, December). УГЛОВАЯ ЗАВИСИМОСТЬ ОДНОФОТОННЫХ МЕЖЗОННЫХ ЛИНЕЙНОЦИРКУЛЯРНЫХ ДИХРОИЗМОВ В КРИСТАЛЛАХ. In The 12 Th International Scientific And Practical Conference "Eurasian Scientific Discussions"(December 18-20, 2022) Barca Academy Publishing, Barcelona, Spain.
13. Расулов, В. Р., Расулов, Р. Я., Муминов, И. А., Эшболтаев, И. М., & Кучкаров, М. (2021). МЕЖДУЗОННОЕ ТРЕХФОТОННОЕ ПОГЛОЩЕНИЕ В InSb.
14. Rasulov, V. R., Rasulov, R. Y., Axmedov, B. B., Muminov, I. A., & Polvonov, B. Z. (2020). Linear-circular dichroism of one-photon absorption of light in narrow-zone semiconductors. contribution of the effect of coherent saturation. European Science Review, (7-8), 49-53.
15. Rasulov, V. R., Rasulov, P. Y., Eshboltaev, I. M., & Sultonov, R. R. (2020). Size Quantization in n-GaP. Semiconductors, 54, 429-432.
16. Расулов, В. Р., Расулов, Р. Я., Султонов, Р. Р., & Ахмедов, Б. Б. (2020). Теоретическое исследование спин-зависимого размерного квантования в двухбарьерной полупроводниковой структуре. «Узбекский физический журнал», 22(1), 16-19.
17. Rustamovich, R. V., Yavkachovich, R. R., Rustamovich, S. R., Mamirjonovich, E. I., & Bahromovich, A. B. (2020). Phenomenology of two and three photon linear-circular dichroism of light absorption in p-GaAs. European science review, (1-2), 97-100.

THEORETICAL CALCULATIONS OF THE MAGNETIC FIELD OF HELMHOLTZ COIL

Taylanov Nizom Abdurazzakovich[1], Dehqonova Ohista Kosimjonovna[2]
[1]Jizzakh State Pedagogical University,
[2]Fergana State University,

Abstract: In the present article we have studied the physical properties of a Helmholtz coil that can produce a second-order uniformity field for use in magnetic resonance imaging (MRI) applications. A Helmholtz coil is a device used to create a region of nearly uniform magnetic field. It consists of two identical magnetic coils arranged symmetrically along a common axis, one on each side of the experimental site, separated by a distance equal to the radius of the round coil and the half-length of the side of the square coil. Each coil carries an equal electric current flowing in the same direction. The main goal of this article is to calculate the magnetic field created by Helmholtz coils at any point in space. Mathematical equations are simulated using the MATLAB simulation tool to demonstrate the axial magnetic field generated by one and two loops. The importance of testing electronic devices under the influence of a constant magnetic field is substantiated. The magnetic field created by Helmholtz coils of finite rectangular cross-section is investigated. An analytical expression is derived for the magnetic field on the axis of a solenoid of finite thickness and the magnetic field on the axis of Helmholtz coils of rectangular cross-section. In the particular case of using Helmholtz coils with a square cross-section, the condition for the second derivative of the magnetic field to vanish along the symmetry axis of the system at its center is numerically analyzed. This makes it possible to determine the distance between square coils at which the field in the center of the system is most uniform. It is shown that taking into account the finiteness of the cross-section

leads to a change in the optimal distance between the coils. A table of optimal distances for square Helmholtz coils of different thicknesses has been compiled.

Keywords: electronic devices, magnetic field, Helmholtz coil effect, rectangular cross-section, round Helmholtz coil; radio frequency coils; modeling; modeling; MATLAB; electromagnetic field measurement; impedance measurements; MRI

Introduction. A Helmholtz coil is a device used to create an area of nearly uniform magnetic field [1-2]. It consists of two identical round magnetic coils located symmetrically, one on each side of the experimental site along a common axis, at a distance d equal to the radius R of the coil. The currents in the coils are equal and flow in the same direction. There are several variations in coil topology, including the use of rectangular coils and different numbers of coils. However, the standard model is the two-coil Helmholtz pair, whose coils are round in shape and have flat sides. In such a device, an electric current is passed through coils to create a fairly uniform magnetic field. Helmholtz coils are used for a variety of purposes. They were used in an argon tube experiment to measure the charge to mass ratio of electrons [3]. They are often used to measure the strength and fields of permanent magnets [4-5]. To do this, a pair of coils is connected to a flux meter, a device that contains the sense coils and electronics that evaluate the change in voltage across the sense coils to calculate the total magnetic flux. In some applications, a Helmholtz coil is used to neutralize the Earth's magnetic field, creating an area with magnetic field strength close to zero. This can be used to see how electric charges and magnetic fields act when they are not affected by the gravitational pull of the Earth or other celestial bodies [6-7]. This work focuses on Helmholtz-type radiofrequency coils that can be used for magnetic resonance imaging applications. In particular, the design, modeling of a circular Helmholtz coil for magnetic resonance imaging, in addition to ensuring good uniformity of the radio frequency electromagnetic field, provides a certain ease of implementation. This work examines the magnetic field of Helmholtz coils - two coaxially located identical radial coils, the distance between the centers of which is equal to their average radius. In the center of the system there is a zone of uniform magnetic field. They are used to obtain a constant, alternating or pulsed magnetic field with a homogeneity zone, which is usually used in experiments, as well as for calibrating magnetic induction sensors, magnetizing and demagnetizing permanent magnets, demagnetizing steel workpieces, parts and tools. The main purpose of this article is to calculate the magnetic field produced by coils at any point in space, and to show and compare the uniform magnetic field produced by a circular Helmholtz coil. Mathematical equations are simulated using the MATLAB simulation tool to demonstrate the axial magnetic field generated by one and two loops.

The Helmholtz coil. Consider a circular Helmholtz coil of radius R , separated by a distance l, as shown in Figure 1. Each coil carries a constant current I in the same direction. Let the magnetic field Bi be calculated on an axis at a distance z from the center of one coil.

The magnetic fields produced by a circular wire loop can be obtained according to the following procedure. Electromagnetic (EM) fields generated by a circular wire loop carrying a current I will satisfy Maxwell's equations. For a wire loop (or coil) excited by a low-frequency current, almost all the energy is stored in the magnetic field. This energy is determined from the concepts and rules of circuit theory.

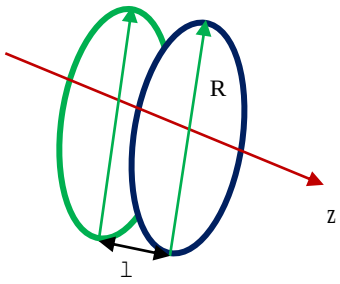

Fig.1. Helmholtz coil arrangement with elliptic loops.

Circuit theory can be thought of as a description of a special class of solutions to Maxwell's equations that result from using the first term of a power series solution for fields. Fields calculated using this approximation are called quasi-static. In the quasi-static approximation, electromagnetic phenomena such as radiation are neglected.

Geometry of the problem. A general rule of thumb for circuit elements driven by sinusoidal voltage or current is that the quasi-static approximation will be extremely good when the physical size of the element is small enough compared to the source excitation wavelength. This limitation will be met if the phase of the voltage (current) is approximately the same over the spatial extent of the element. For a circular loop, this condition requires that the current be nearly constant around the circumference of the loop. The current can change over time, but at each moment of time the current in each part of the circuit must have the same value. Therefore, the quasi-static approximation will be very good as long as $2\pi a \ll \lambda$ (or in terms of frequency instead of wavelength, $\nu \ll c/10a$, where a is the radius of the loop and c is the speed of light in free space. One can find the electromagnetic fields produced by a loop in this order of approximation by determining the current in the loop using circuit theory and using this uniform current as a source of vector potential from which the fields can be easily derived. This is the approach used below.

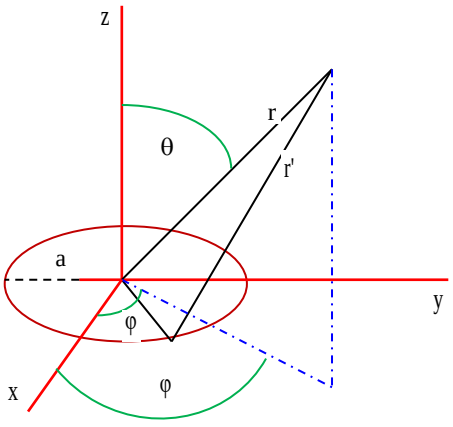

Fig.2. Elliptic coil arrangement to compute the off-axis magnetic field.

In Fig. Figure 2 shows the coordinates and variables for a loop of radius a located in the xy plane . The circuit is assumed to have a total current I.

Basics of electromagnetism. Since we will be working extensively with electromagnetism, it is important that we establish a good foundation for the work. This benchmark will be described by the famous Maxwell equations formulated in 1861 [7], which are given below:

$$\vec{\nabla} \times \vec{E} = -\frac{\partial \vec{B}}{\partial t}, \qquad (1)$$

$$\vec{\nabla}\times\vec{B}=\mu_0\left(\vec{J}+\varepsilon_0\frac{\partial\vec{E}}{\partial t}\right), \quad (2)$$

$$\vec{\nabla}\cdot\vec{E}=\frac{\rho}{\varepsilon_0}, \quad (3)$$

$$\vec{\nabla}\cdot\vec{B}=0. \quad (4)$$

where E and B represent the electric and magnetic fields, respectively; electric ε_0 and μ_0 magnetic permeability in vacuum, respectively; and J current density. Although Maxwell's equations do describe our structure, they can be difficult to work with. For our work it will be useful to use Biot-Savart's law, which is given here below:

$$\vec{B}(\vec{r})=\frac{\mu_0}{4\pi}\int_C\frac{Id\vec{l}\times(\vec{r}-\vec{r}\,')}{|\vec{r}-\vec{r}\,'|^3}. \quad (5)$$

where C is the path along the direction of the current I, r and r' are vectors representing the distance between the origin and the place where the field is calculated, and the current element, respectively. Looking at Maxwell's second equation (2) and remembering the following property of divergence:

$$\nabla\cdot(\nabla\times\vec{A})=0. \quad (6)$$

let us introduce the vector magnetic potential A :

$$\vec{B}=\nabla\times\vec{A}, \quad (7)$$

which may seem tedious, but as we will see, it will be useful for multipolar extensions. Using equations (3) and (4), we obtain the expression for the magnetic vector potential:

$$\vec{A}(\vec{r})=\frac{\mu_0 I}{4\pi}\int\frac{d\vec{r}\,'}{|\vec{r}-\vec{r}\,'|}. \quad (8)$$

where A is the vector potential, and I is the current in the circuit. From the direction of the current A has only a φ and by symmetry A does not depend on the variable φ. When setting up the integration, we use arbitrary values $\varphi=0$ to simplify the results. Using the symbols shown in Figure 2 , we may get the following relations

$$d\vec{l}=(-a\sin\varphi',a\cos\varphi',0)d\varphi',$$
$$\vec{r}=(r\sin\theta,0,r\cos\theta),$$
$$\vec{r}=(a\cos\varphi',a\sin\varphi',0),$$
$$|\vec{r}-\vec{r}\,'|=\sqrt{r^2+a^2-2r\cdot a\cdot\sin\theta,\cos\varphi'}. \quad (9)$$

The distribution of magnetic field. Substituting these variables into the integral, we notice that the integral with participation $\sin\varphi'$ vanishes (it is odd), as it should be, since A_φ only the component must survive, and the integral with $\cos\varphi''$ (even) allows us to reduce the range of integration by half. It leads to

$$A_\varphi=\frac{\mu_0 Ia}{2\pi}\int_0^\pi\frac{\cos\theta d\theta}{\sqrt{\rho^2+R^2-2\rho R\sin\theta\cos\theta}}. \quad (10)$$

$$A_\varphi(\rho,0,z)=\frac{\mu_0}{4\pi}\int_0^{2\pi}\frac{IR(-\sin\theta e_\theta+\cos\theta e_\theta)d\theta}{\sqrt{\rho^2+R^2+z^2-2\rho\cos\theta}} \quad (11)$$

It is more convenient to express this integral in terms of cylindrical coordinates, using $r^2 = \rho^2 + z^2$ $\sin\theta = \dfrac{\rho}{\sqrt{\rho^2 + z^2}}$

$$A_\varphi(\rho, z) = \frac{\mu_0 IA}{2\pi} \int_0^\pi \frac{\cos\theta d\theta}{\sqrt{\rho^2 + R^2 + z^2 - 2\rho R\cos\theta}}. \quad (12)$$

This integral does not have a closed form; however, there is a conversion that results in table functions. Change the variable to obtain the upper limit of the integral $\pi/2$ using $\varphi' = \pi + 2\varphi$. The integral becomes

$$A_\varphi(\rho, z) = \frac{\mu_0 IA}{2\pi} \int_0^{\pi/2} \frac{(2\sin^2\theta - 1)d\theta}{\sqrt{(\rho + R)^2 + z^2 - 4\rho R\sin^2\theta}}. \quad (13)$$

If we define $k^2 = \dfrac{4ar}{(a + r)^2 + z^2}$, then the integral transforms into

$$A_\varphi(\rho,\varphi) = \frac{\mu_0 I}{\pi k}\sqrt{\frac{a}{\rho}}\left[\left(1 - \frac{k^2}{2}\right)K - E\right]. \quad (14)$$

An accurate (numerical) calculation of the off - axis magnetic field of a circular loop can be started from the vector potential in spherical coordinates given in (14). An alternative is to turn to elliptic integrals: introducing cylindrical coordinates $z = \rho\sin\theta$, $r = \rho\cos\theta$, and the parameter $k^2(z, r) = \dfrac{4ar}{(a + r)^2 + z^2}$, from (14), after simple transformations we obtain

$$K((k) = \int_0^{\pi/2} (1 - k^2\sin^2\gamma)^{-1/2} d\gamma,$$
$$E(k) = \int_0^{\pi/2} (1 - k^2\sin^2\gamma)^{1/2} d\gamma \quad (15)$$

K is a complete elliptic integral of the first kind, E and is a complete elliptic integral of the second kind. Both functions are tabular. Magnetic fields are calculated from the vector potential by $B = \nabla \times A$, providing two components:

$$B_\rho(\rho, z) = -\frac{\partial A_\varphi}{\partial z}, \quad B_z(\rho, z) = \frac{1}{\rho}\frac{\partial}{\partial z}(\rho A_\varphi). \quad (16)$$

The final expression for the magnetic field components takes the form

$$B_\rho(\rho,z) = \frac{\mu_0 I}{2\pi}\frac{z}{\sqrt{\left[(a + \rho)^2 + z^2\right]}}\left[\frac{a^2 + \rho^2 + z^2}{(a - \rho)^2 + z^2}E - K\right]. \quad (17)$$

$$B_z(\rho,z) = \frac{\mu_0 I}{2\pi}\frac{z}{\sqrt{\left[(a + \rho)^2 + z^2\right]}}\left[\frac{a^2 - \rho^2 - z^2}{(a - \rho)^2 + z^2}E - K\right]. \quad (18)$$

For small values of k (i.e. $r \gg a$ or $r \ll a$) of the expansion

$$K = \frac{\pi}{2}\left(1 + \frac{k^2}{2} + \frac{9}{64}k^4 + ...\right), \quad E = \frac{\pi}{2}\left(1 - \frac{k^2}{2} - \frac{9}{64}k^4 + ...\right), \quad (19)$$

For a single loop in the xy plane , we can find the magnetic field components at any location ρ and z by first determining k from the definition above and then substituting into the above formulas. We can check the accuracy of these expressions for the simple case of magnetic field components along the loop axis. On the axis $\rho = 0$, from which follows k = 0 and, therefore, $K(0) = E(0) = \pi/2.$ the expression for B_ρ becomes undefined, but applying L'Hopital's rule gives $B_\rho = 0$. Expression for B_z becomes

$$B_z = \frac{0.5\mu_0 I}{\sqrt{(a^2 + z^2)^3}} \tag{20}$$

as expected. To calculate the magnetic fields from the Helmholtz coil, fields calculated for two circuits having the same axis, located in planes in $z = -d$ and $L = d$. The separation distance 2 d is related to the loop radius by the relation $d = a/2$. The expression for the total magnetic field, written in terms of the above derivation, is simply the sum of the individual fields from each loop .

Numerical results. In Fig. Figure 3 shows the axial B_z (left) and radial B_ρ (right) field components along the vertical axis of the hole. We see that the BZ shows three humps due to the three-turn configuration. The field is within 10% of the central value between Z = 0.8 and 3.1 m. The radial component B_ρ, shown below, rolls off below 1 and above 3 m. Here the 10% margin is achieved at approximately Z = 0.8 and 3 ,1 m. The decrease in the radial field is accompanied by an increase in the axial field, which increases the “undesirable” component of the BZ field below 1 and above 3 m. We cannot do anything about this decrease except increase the radius of the turns or add additional turns. The decision on how far to lower the resonator into the “poor field” region depends on the gradient and the dependence of the damping limits on the magnetic field.

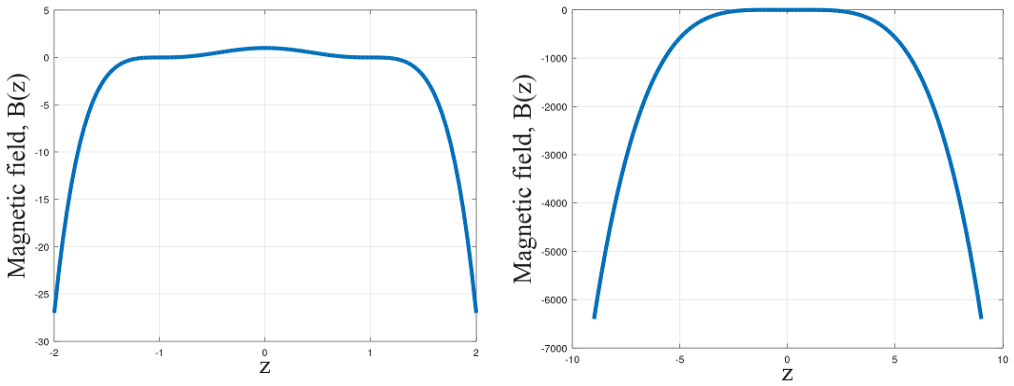

Fig . 3. A two- dimensional comparison of the measured and calculated magnetic field as a function of z at the center line ($\rho = 0$).

Figure 4 is another representation of the same data, presented as contour plots. Contour plots show that the field is uniform at 1.3 x 10^{-6} T for most of the inner region.

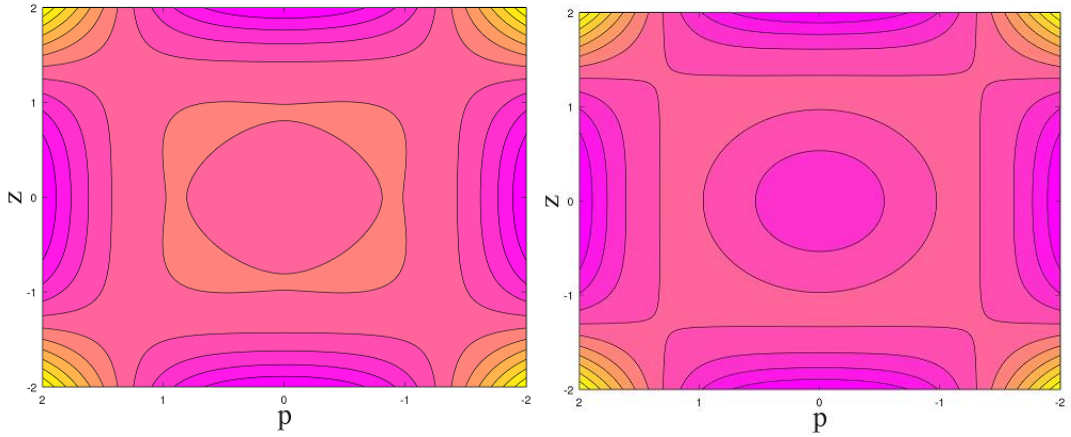

Fig . 4. A two- dimensional comparison of the measured and calculated magnetic field as a function of z at the center line ($\rho = 0$).

In Fig . Figure 5 shows a three-dimensional comparison of the measured and calculated z-components of the magnetic field depending on ρ and z for .for typical parameter values $LN = 50,\ \mu_0 = 4\pi e^7,\ I = 0.019,$

$a = 0.155,\ d = 1.19/2.$ You can see that they compare very well in terms of wave shape and magnitude.

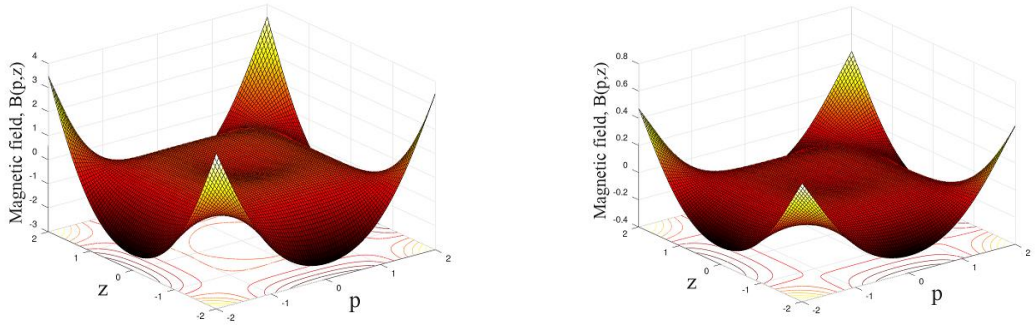

Fig.5. A 3D graph of the magnetic field B(ρ,z) at different values of parameter a

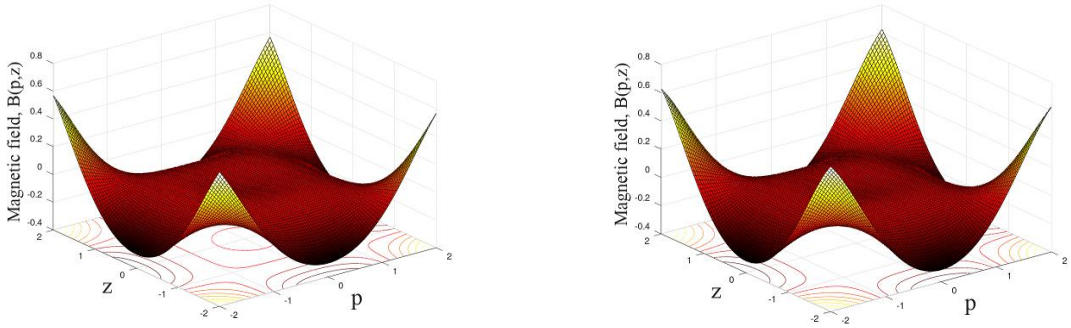

Fig.5. A 3D graph of the magnetic field B(ρ,z) at different values of parameter a

CONCLUSION

The present work examines and demonstrates the performance of standard square and round Helmholtz coils that can be used for magnetic resonance imaging. The coil assembly consists of two coaxial loops separated by a distance equal to their radius for a round coil and half the side length for a square coil, and carrying the same current (co-current mode) in a symmetrical arrangement. The developed Helmholtz-type coils create a uniform second-order field. A comparative study of MATLAB simulation along with experimental implementation was conducted to test the magnetic field uniformity of round and square Helmholtz coils. The magnetic field value for which the coil was designed was successfully achieved. The Helmholtz coil is an excellent source of uniform magnetic field and it was built within a very economical budget. It was noticed that if the radius of the round coil is equal to the side of the square, and the distance between the coils is less than 50% of the radius of the round coil and less than 55.4% of the side of the square coil, then the sensitivity of the magnetic field for a round coil is greater than for a square coil . But a pair of square coils exhibits greater magnetic field uniformity than a pair of round coils. It was also observed that the distance between the turns should be approximately equal to 50% of the radius for a round coil and 27.7% of the side length for a square Helmholtz coil. A pair of square Helmholtz coils demonstrated greater field uniformity than round Helmholtz coils, which is desirable for MRI applications. It has been established that the sensitivity (magnitude) of the magnetic field in a pair of round Helmholtz coils is greater than that of square coils.

REFERENCES

[1] F. Romeo, D. I. Holt, “Magnetic Field Profiling: Analysis and Adjustment of Coil Design,” Magnetic Resonance in Medicine, Vol . 1, No. 1, pp. 44-65, 1984

[2] CE Hayes , WA Edelstein , J.F. Schenck , O.M. Mueller , M. _ Eash , "Efficient, Highly Uniform RF Coil for Whole-Body NMR Imaging at 1.5 T", Journal of Magnetic Resonance , Vol . 63, pp. 622-628, 1985.

[3] L. Guendouz, S. M. Ghaly, A. Hedgej, J. M. Escanier, D. Canet, “Improved Helmholtz-type magnetic resonance imaging coils with spherical and ellipsoidal four-coil systems with high B 1 uniformity , ” "Magnetic Resonance Concepts", Vol. 33B, No. 1, pp. 9-20, 2008

[4] K. Asher, N.K. Bangerter, R.D. Watkins, G.E. Gold, “Radiofrequency Coils for Musculoskeletal MRI,” Issues in Magnetic Resonance Imaging, Vol . 21, No. 5, pp. 315-323, 2010

[5] SMA Ghaly , L. _ Guendouz , A. _ Hedjiedj , J.M. Escanye , D. _ Canet , "Improved Helmholtz-Type Coils with High Uniformity B 1 - Spherical and Ellipsoidal Configurations", 24th IASTED International Multi-Conference on Biomedical Engineering, Innsbruck, Austria, 15-17 February 2006.

[6] S. Li, Q. X. Yang, M. B. Smith, "RF Coil Optimization: Estimating B 1 Field Uniformity Using Field Histograms and Finite Element Calculations", Magnetic Resonance Imaging, Vol . 12, No. 7, pp. 1079-1087, 1994

[7] B. Gruber, M. Freling, T. Leiner, D. W. J. Klomp, “RF Coils: A Practical Guide for Nonphysicists,” Journal of Magnetic Resonance, Vol . 2018. T. 48, No. 3. P. 590-604.

[8] J. Mispelter, M. Lupu, A. Brighe, NMR probes for biophysical and biomedical experiments, theoretical principles and practical recommendations, 1st edition, Imperial college Press , 2006